SCIENCE CHINA
Chemistry

•INVITED REVIEWS•

August 2018 Vol.61 No.8: 979–992
https://doi.org/10.1007/s11426-018-9337-4

Controllable macrocyclic supramolecular assemblies in aqueous solution

Yong Chen[1,2], Feihe Huang[3], Zhan-Ting Li[4] & Yu Liu[1,2*]

[1]*State Key Laboratory of Elemento-Organic Chemistry, College of Chemistry, Nankai University, Tianjin 300071, China;*
[2]*Co-Innovation Center of Chemistry and Chemical Engineering (Tianjin), Tianjin 300072, China;*
[3]*State Key Laboratory of Chemical Engineering, Center for Chemistry of High-Performance & Novel Materials, Department of Chemistry, Zhejiang University, Hangzhou 310027, China;*
[4]*Department of Chemistry, Shanghai Key Laboratory of Molecular Catalysis and Innovative Materials and Collaborative Innovation Centre of Chemistry for Energy Materials (iChEM), Fudan University, Shanghai 200438, China*

Received July 2, 2018; accepted July 19, 2018; published online July 25, 2018

A series of macrocycles, including crown ethers, cyclodextrins, calixarenes, pillararenes and cucurbiturils, are well known to be able to associate various organic/inorganic/biological guest molecules and ions in their well-defined cyclic cavities to form stable host-guest complexes and supramolecular systems through the cooperative contributions of various non-covalent interactions. When one or more functional groups are attached to the cavity of macrocycles or guest molecules, enhanced and/or controlled host-guest associations may take place, leading to not only improved host-guest binding abilities but also fascinating properties. In this review, some representative contributions in the construction of controllable macrocyclic supramolecular assemblies in aqueous solution are presented with an emphasis on the stimuli-responsive control manner and wide applications of this property.

macrocycle, supramolecular assembly, stimuli-responsive, aqueous solution

Citation: Chen Y, Huang F, Li ZT, Liu Y. Controllable macrocyclic supramolecular assemblies in aqueous solution. *Sci China Chem*, 2018, 61: 979–992, https://doi.org/10.1007/s11426-018-9337-4

1 Introduction

Within the field of supramolecular chemistry there is an increasing interest focused on the potential applications of macrocycles including crown ethers, cyclodextrins, calixarenes, pillararenes and cucurbiturils (Scheme 1). With rigid and well-defined structures and, most of all, cyclic cavities, these macrocycles can bind various inorganic/organic/biological molecules and ions in both solution and the solid state, and are thus extensively employed as not only excellent receptors for molecular recognition but also convenient building blocks to construct nanostructured functional materials [1].

It is noteworthy that macrocyclic supramolecular systems possess several inherent advantages. Firstly, superior to the traditional organic synthesis of covalent systems that usually requires a large amount of organic solvents, a long time course or special instruments and does harm to the environment, macrocyclic supramolecular systems can be conveniently prepared through cooperative contributions of several intermolecular non-covalent interactions such as van der Waals, hydrophobic, hydrogen bonding, and electrostatic interactions by mixing macrocycle and model substrate components in solution. Secondly, the non-covalent association of macrocycles with substrates enables the close contact of the host and guest in space, which will consequently strengthen the supramolecular interactions owing to the short distance between the host and guest. Thirdly,

*Corresponding author (email: yuliu@nankaieducn)

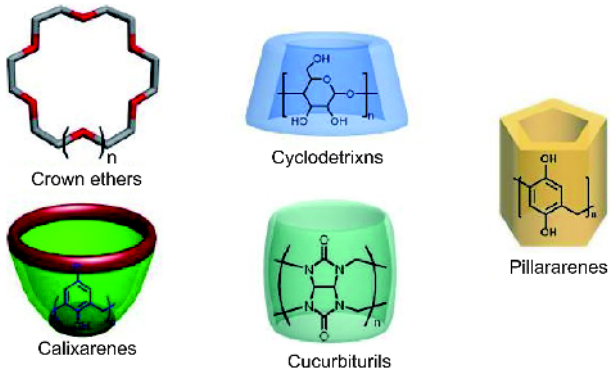

Scheme 1 Structures of macrocycles (color online).

macrocyclic supramolecular systems usually bear more than one functional groups that can simultaneously interact with the accommodated substrates, which is expected to improve the properties of building blocks through an integrated effect. As a joint result of these factors, macrocyclic supramolecular systems can exhibit fascinating properties.

During the period of the 1970s through the beginning of the 2000s, many successful studies on the controllable macrocyclic supramolecular systems were reported [2]. The charge transfer between electron-deficient 4,4′-bipyridinium derivatives and electron-rich aromatic rings are extensively used to construct mechanically interlocked molecules such as rotaxanes and catenanes and to enable the controllable molecular motions [3]. Moreover, the supramolecular system by dibenzo-24-crown-8 and a linear substrate with an axle component bearing an *N*,*N*-dimethylaniline group on the 4-position of the pyridinium ring performed a threading/dethreading motion through switching off/on the intramolecular charge-transfer (ICT) process [4]. Similarly, another supramolecular system comprised of a dibenzo-24-crown-8 derivative bearing a terpyridine unit as a chelator for lanthanide ions and a ferrocene-containing or fullerene-containing ammonium salt also exhibited the reversibly governed fluorescence emissions [5]. In addition, numerous controllable molecular devices, including molecular machines and switches [6,7], molecular keypad lock [8], fluorescent chemosensor [9,10], fluorescent gel [11], based on macrocyclic supramolecular systems were also reported, which can be smartly controlled by solvent, redox [12], acid/base [13], and so on. However, the relatively low water solubility of many macrocycles greatly limits their application in many fields, especially in biological science, because many important biological processes mainly occur in aqueous environment. Therefore, many efforts are contributed to the construction of controllable water-soluble macrocyclic supramolecular systems and to exploring their application potential. This review summarizes our recent endeavors on the water-soluble macrocyclic supramolecular systems constructed from crown ethers, cyclodextrins, calixarenes, pillararenes and cucurbiturils (Scheme 1), with a special emphasis on their controllable assembly/disassembly, morphological conversion and properties in aqueous environment.

2 Crown ether-based supramolecular assembly

Crown ethers are a class of macrocyclic compounds that consist of a ring containing several ether groups [14]. The most common crown ethers are ethyleneoxy oligomers, wherein the oxygen atoms are well situated to coordinate with a cationic substrates located at the interior of the ring. Therefore, crown ethers become the simplest and most widely used host molecules for both metallic and organic cations. Generally, most of crown ethers are water insoluble, and water soluble crown ethers, such as 18-crown-6 and 24-crown-8, only display weak affinity with guest due to that water molecules not only strongly interfere the ion-dipole interaction between crown ethers and guest molecules, but also are unfavorable for entropy change due to the flexible and low preorganized polyethyleneoxy chain. In 2008, Loeb and Nikitin *et al.* [15] dramatically enhanced the solubility of crown ether in highly polar solvents by introducing anionic groups SO^{3-} or COO^{-} to crown ether. Using this method, crown ether-based controllable supramolecular systems are successfully constructed in water. In a typical example of light-controlled reversible formation and dissociation of nanorods via interconversion of sulfonatocrown ether-based pseudorotaxanes, four components, i.e., tetrasulfonated 1,5-dinaphtho-32-crown-8, 1-methyl-1′-dodecyl-4,4′-bipyridinium bromide iodide, 4,4′-azodibenzoic acid and α-cyclodextrin were included in aqueous solution. Spectroscopic and microscopic studies demonstrated that nanorods were formed by the self-assembly of the amphiphilic [2]pseudorotaxane between tetrasulfonated 1,5-dinaphtho-32-crown-8 and 1-methyl-1′-dodecyl-4,4′-bipyridinium. Therein, the hydrophobic chains interlaced with each other in the middle of the nanorod, whereas hydrophilic sulfonate groups surrounded the surface of the nanorod. On the other hand, because the alkyl chain could be encapsulated by α-cyclodextrin with moderate binding constants, α-cyclodextrin could be utilized to modulate the assembly of [2]pseudorotaxane, leading to the formation of tetrasulfonated 1,5-dinaphtho-32-crown-8/1-methyl-1′-dodecyl-4,4′-bipyridinium/α-cyclodextrin [3]pseudorotaxane. Furthermore, 4,4′-azodibenzoic acid was selected as a competitive guest to dissociate the [3]pseudorotaxane owing to the stronger binding ability of α-cyclodextrin with 4,4′-azodibenzoic acid than with 1-methyl-1′-dodecyl-4,4′-bipyridinium. Interestingly, upon irradiation of the four-component solution with 365 nm, the interconversion from *trans*-4,4′-azodibenzoic acid to *cis*-azodibenzoic acid occurred, leading to the dis-

sociation of 4,4′-azodibenzoic acid/α-cyclodextrin complex and the formation of [3]pseudorotaxane. Accordingly, the transformation of nanorods into nanoparticles was observed in the TEM images. More interestingly, upon subsequent irradiation of the four-component solution with 450 nm, the spectroscopic behaviors reverse to their original state, and nanorods reappeared in TEM images. Benefiting from the inherent photoisomerization of 4,4′-azodibenzoic acid, the reversibility of photo-induced interconversion from [3]pseudorotaxane to [2]pseudorotaxane could be completed over three cycles. Therefore, the reversible assembly and disassembly processes were expected to be driven by azobenzene photoisomerization in the four-component solution (Figure 1) [16].

Using a similar method, another crown ether-based supramolecular system was successfully constructed in water as a light-controlled [3]pseudorotaxane [17]. Herein, a supramolecular assembly was constructed from the inclusion complex of an azobenzene-containing pyridinium salt with α-cyclodextrin and tetrasulfonated 1,5-dinaphtho-32-crown-8 (Figure 2). By employing the molecular recognition of azobenzene-containing pyridinium with α-cyclodextrin and tetrasulfonated 1,5-dinaphtho-32-crown-8, a multicomponent [3]pseudorotaxane was constructed. In addition, [3]pseudorotaxane could be further reversibly switched to [2]pseudorotaxane upon photoirradiation. Interestingly, the motion of the macrocyclic host in [3]pseudorotaxane exhibited a guest-mediated response, that is, once the azobenzene guest was modified with the doubly-charged bis(pyridinium) terminal groups, instead of the singly-charged pyridinium units, the photoisomerization of *trans*-azobenzene could no longer be converted into the cisisomer in the presence tetrasulfonated 1,5-dinaphtho-32-crown-8 of and α-cyclodextrin. It is noteworthy that this light-controlled [3]pseudorotaxane through the supramolecular cooperativity

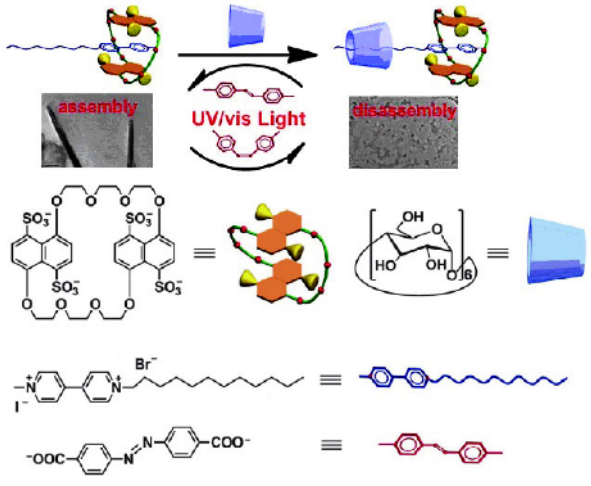

Figure 1 Self-assembly/disassembly based on the photoresponsive interconversion of crown ether-based pseudorotaxanes (color online).

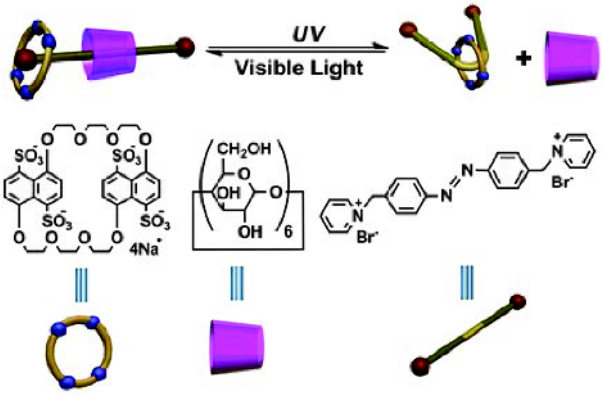

Figure 2 Interconversion process of different types of pseudorotaxanes with tetrasulfonatocrown ether and α-cyclodextrin in water (color online).

of an azobenzene-pyridinium conjugate with two different types of water-soluble macrocyclic receptors, i.e., tetrasulfonatocrown ether and cyclodextrin, in aqueous solution, and the formation of this ternary assembly was driven by the combination of the hydrophobic interaction of α-cyclodextrin with trans-azobenzene and the electrostatic attraction between the tetrasulfonatocrown ethers and the singly-charged pyridinium salt. Upon the photoisomerization of the azobenzene group from its trans to cis isomer, the α-cyclodextrin unit was released from the molecular axle, and the crown ether ring slided from the pyridinium terminal group to the azobenzene group in the center.

The binding affinity of guest with different macrocyclic receptors, such as cucurbituril, pillararene, and tetrasulfonatocrown ether, was also used to control the topological features of supramolecular assemblies (Figure 3) [18]. Without macrocyclic receptors, bipyridinium-modified diphenylalanine existed as fine nanofibers with 20 nm diameter. However, diverse self-assembled nanostructures were obtained by mixing bipyridinium-modified diphenylalanine with equimolar macrocyclic hosts in aqueous solution. That is, bipyridinium-modified diphenylalanine formed a number of nanorods (length 500 nm and width 200 nm) with CB[7], octahedron-like structures at the micrometer scale with CB[8], right-handed helical nanowires (diameters 600 nm) with water-soluble pillar[5]arene, and rectangular nanosheets (length ranging from 200 to 700 nm) with tetrasulfonated 1,5-dinaphtho-32-crown-8. These microscopic investigation results demonstrate that the addition of macrocyclic compounds could dramatically influence the spatial alignment of diphenylalanine and then induce a broad range of morphological variation from nanofibers to nanorods, octahedron-like nanostructure, helical nanowires, and rectangular nanosheets. On the other hand, the addition of CB[8] or tetrasulfonated 1,5-dinaphtho-32-crown-8 as competitive host to the CB[7]- or pillar[5]arene-based assembly triggered the morphological changes, indicating the

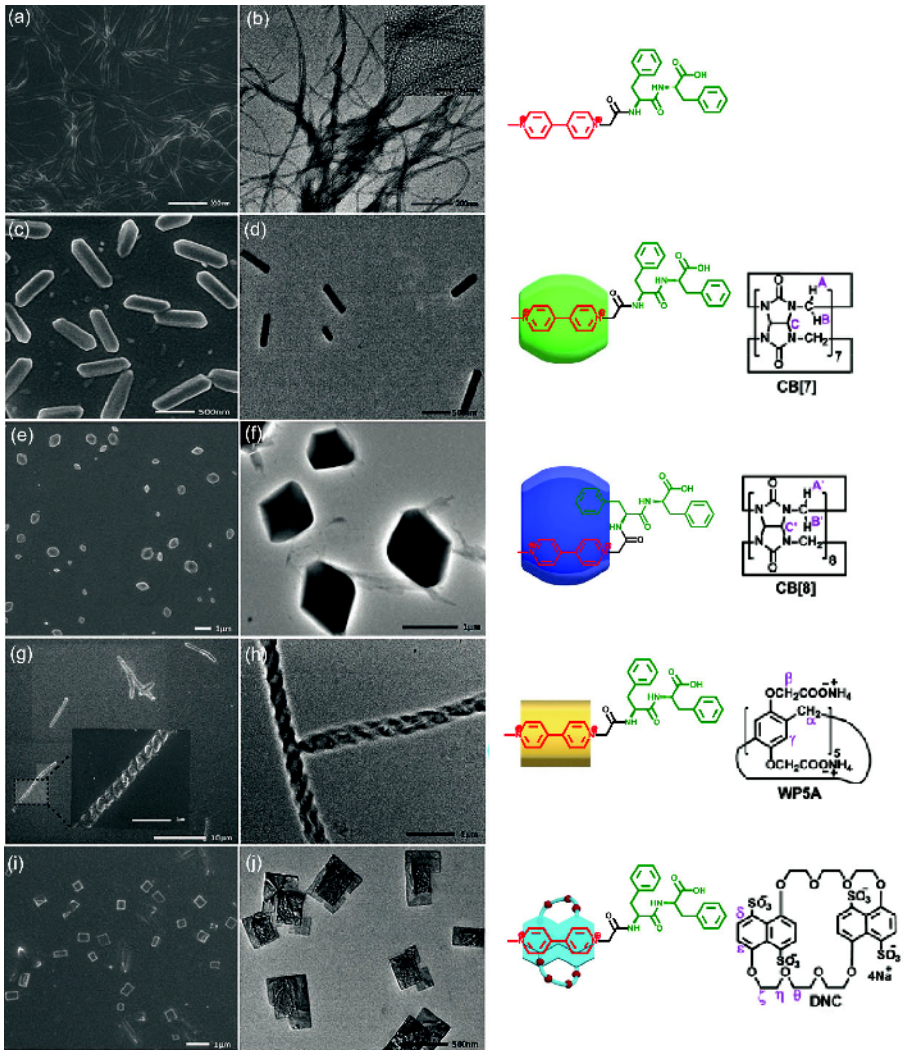

Figure 3 Various morphology controlled by host macrocycles (color online).

K_S-dependent supramolecular assembling behaviors.

3 Cyclodextrin-based supramolecular systems

Cyclodextrins are a class of cyclic oligosaccharides with six-eight *D*-glucose units linked by α-1,4-glucose bonds [19]. The exterior surface of cyclodextrin is hydrophilic, but the cavity of cyclodextrin is hydrophobic. Significantly, the hydrophobic cavity of cyclodextrins, mostly in a truncated cone conformation, mainly bind various neutral or negatively charged substrates, which enable the wide application of cyclodextrins in many fields of science and technology as molecular recognition receptors [20,21], drug delivery carriers [22], biomimetic catalysts [23], and so on. By incorporating energy donor/acceptors to cyclodextrins, cyclodextrin-based supramolecular systems with energy transfer properties can be constructed. A typical example comes from a water-soluble supramolecular assembly constructed form an anionic cyclic polysaccharide, sulfato-β-cyclodextrin (SCD), an aggregation-induced emission (AIE) molecule, oligo(phenylenevinylene) derivative (OPV-I), and a fluorescent dye, nile red (NiR), where the SCD/OPV-I acted as the donor and NiR acted as the acceptor (Figure 4) [24]. There are several advantages of this system as (1) at a high concentration, OPV-I possessed the good AIE properties, (2) SCD could greatly lower the critical aggregation concentration (CAC) of OPV-I, thus improving the AIE properties of OPV-I and enabling the good water solubility of resultant light-harvesting system, (3) the hydrophobic dye NiR could be loaded in the hydrophobic layer of OPV-I/SCD supramolecular assembly. Without SCD, OPV-I emitted the strong yellow fluorescence when excited at 365 nm, owing to the AIE of OPV-I. With the addition of SCD, the fluorescence intensity of OPV-I increased 3.7 times, and the fluorescence enhancement was clearly observed by the naked eye. Moreover, the CAC value of OPV-I decreased 4.8 times with the addition of SCD, and the preferable molar

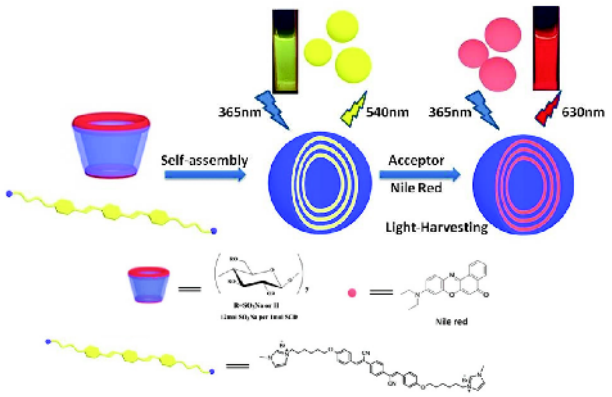

Figure 4 Cyclodextrin-based light-harvesting system (color online).

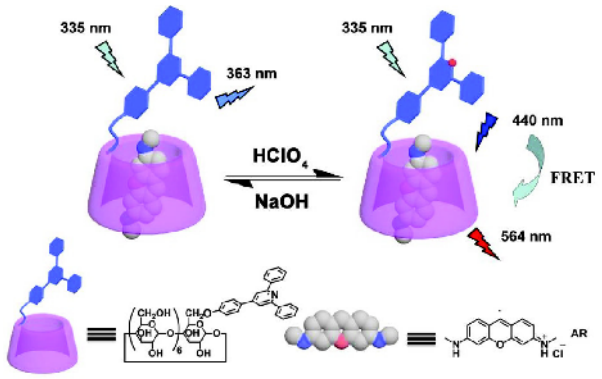

Figure 5 Controlled energy transfer within triarylpyridine-cyclodextrin/acridine red supramolecular system (color online).

ratio for the supramolecular assembly was SCD:OPV-I=1:6. The TEM and SEM images of SCD:OPV-I assembly showed several spherical nanoparticles with diameters ranging from 50 to 150 nm. Therefore, a possible assembly mode was deduced as follows: free OPV-I molecules could not form a large self-aggregate. Upon the addition of SCD, one SCD and several OPV-I formed a complex. Subsequently, various complexes integrated together to form a large multilayer aggregate that curved to generate a multilayer sphere with alternating shell structure. The resulting aggregates were simultaneously stabilized by several noncovalent interactions, including host-guest, electrostatic, and π-π interactions, and the synergetic contribution of these noncovalent interactions endowed the OPV-I molecules with good aggregation stability, short aggregation distance, and a high-order degree of aggregation. Furthermore, NiR could be loaded into the hydrophobic layer of the OPV-I/SCD assembly, the fluorescence of OPV-I/SCD (donor) decreased, but the fluorescence emission of NiR (acceptor) increased when excited at 365 nm. The bright-red fluorescence assigned to the emission of NiR was readily observed by the naked eye even in the presence of a trace mount of NiR (donor/acceptor ratio up to 1500:1). Through a simple calculation, the energy-transfer efficiency was calculated as 72%, and the antenna effect was calculated to be 32.5 at a donor/acceptor ratio of 125:1.

Significantly, some stimulation-response sites can also be introduced to control the energy transfer of cyclodextrin-based supramolecular systems. In a supramolecular system formed by 2,4,6-triarylpyridine modified β-cyclodextrin and acridine red, acridine red acts as the energy acceptor, and 2,4,6-triarylpyridine acts as not only the energy donor but also the pH-response control site (Figure 5). When 2,4,6-triarylpyridine unit is in neural state, no obvious spectral overlap is observed between the fluorescence emission band of 2,4,6-triarylpyridine and the absorption band of acridine red. However, when adding another portion of $HClO_4$ to the same solution, the fluorescence emission band of protonated 2,4,6-triarylpyridine presents appreciable overlap with the absorption band of acridine red. This spectral overlap between host and guest through long-range dipole-dipole interaction consequently leads to the appearance of an emission at 564 nm when exciting the solution at 335 nm owing to the through-space energy transfer behaviors, and the reversibility of this acid/base-controlled energy transfer can be repeated for several cycles [25].

Besides energy transfer, the morphology of supramolecular assembly can also be smartly controlled. A typical example comes from a photochemically interconvertible supramolecular nanotube-nanoparticle system (Figure 6) constructed through secondary assembling of self-aggregates of amphiphilic porphyrin derivatives mediated by *trans*- and *cis*-azobenzene-bridged bis(permethyl-β-cyclodextrin) [26].

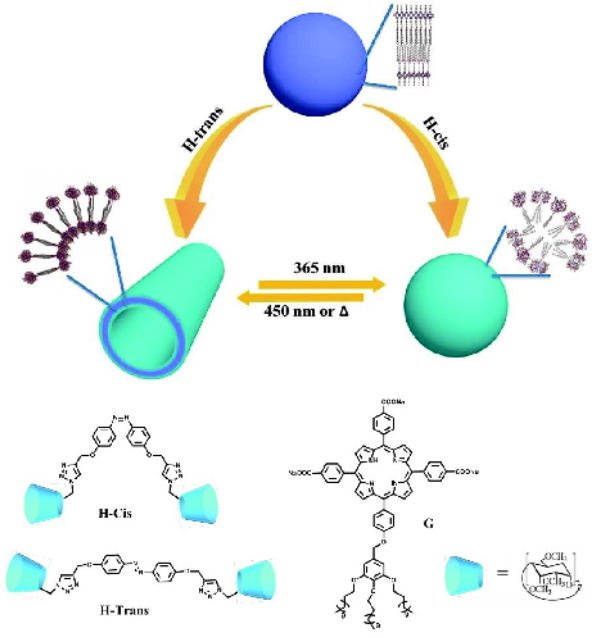

Figure 6 Photo-controlled reversible conversion of nanotube and nanoparticle mediated by cyclodextrin dimers (color online).

Without bridged bis(permethyl-β-cyclodextrin), the free porphyrin formed H-type self-aggregates as spherical nanostructures with an average diameter of 150 nm in aqueous solution. Furthermore, the permethyl-β-cyclodextrin in host could very strongly bind water-soluble porphyrin in aqueous solution. The complexation stoichiometry between monomeric permethyl-β-cyclodextrin and guest porphyrin was determined as 2:1 by Job analysis and the binding constants as K_1=3.4×10^8 M^{-1} and K_2=1.2×10^7 M^{-1} by UV/vis titration. This strong binding enabled the spontaneous secondary assembling upon mixing guest porphyrin and bridged bis(permethyl-β-cyclodextrin) in aqueous solution. SEM images of an air-dried equimolar solution of trans-isomer of bridged bis(permethyl-β-cyclodextrin) and guest porphyrin displayed a number of open-ended, curved tubular structures with large aspect ratios, and the length reached tens of micrometer. Moreover, TEM images clearly showed the hollow tubular structure of a uniform hollow size, and the average inner and outer diameters of the nanotubes were about 45 and 61 nm, respectively, with a wall thickness of about 8 nm. Significantly, after irradiation of the solution of nanotube at 365 nm for 20 min, the long nanotubes turned to a number of solid nanoparticles with an average diameter of 180–200 nm. These nanoparticles were appreciably larger and denser than those formed by the self-aggregation of guest. Therefore, the morphological conversion was deduced to be driven by the photo-induced geometrical change of bridged bis(permethyl-β-cyclodextrin) from the trans-isomer to cis-isomer. That is, under the light irradiation, the trans-isomer units in assembly converted to cis-isomer units, and these cis-isomer units subsequently interacted with guest through sandwich complexation. The resulting cis-isomer/guest sandwich complexes, possessing a larger hydrophilic head than free guest, first self-assembled to small micelles. Then, these micelles further aggregated to form larger nanoparticles. Significantly, this photocontrolled morphological conversion is reversible and recyclable for tens of times.

In another successful example, a photocontrolled, interconvertible supramolecular 2D-nanosheet/1D-nanotube system (Figure 7) was constructed through the supramolecular assembly of adamantanyl-modified diphenylalanine with azobenzene-bridged bis(β-cyclodextrin) [27]. Therein, the adamantanyl moiety could strongly bind with the free β-cyclodextrin cavity in host. Then, two-dimensional planar nanosheets were formed between adamantanyl-modified diphenylalanine and trans-form azobenzene-bridged bis(β-cyclodextrin). The lengths and widths of nanosheets reached several micrometers, and the heights of these thin planar nanostructures were measured as approximately 7 nm by AFM experiments. Interestingly, the assembly between adamantanyl-modified diphenylalanine and cis-form azobenzene-bridged bis(β-cyclodextrin) presented an entirely different morphology as open-ended, curved tubular structures. Owing to the good photoisomerization properties of the azobenzene moiety in host, the 1D-nanotubes and 2D-nanosheets could mutually interconvert via light irradiation at different wavelengths. Typically, after irradiation of the solution of nanosheets with UV light (365 nm) for 10 min, nearly all of the 2D nanosheets converted into 1D-nanotubes. Meanwhile, the formed 1D nanotubes could revert to the original 2D nanosheets upon their subsequent irradiation with visible light (450 nm) for 30 min. Interestingly, when irradiating the solution of nanosheets for a short time, a number of open nanotubes were formed. After lengthening the irradiation time, these nanotubes converted into closed ones. Therefore, we can reasonably deduce the possible assembly modes: two host-guest complexes firstly form end-to-end dimers, and then these dimers further self-assemble to bilayer nanosheets or nanotubes through a secondary assembly process. Under UV light irradiation, the planar nanosheets with a bilayer structure bend into nanotubes, while the as-formed nanotubes can revert to nanosheets under visible light irradiation. Significantly, the photocontrolled 2D nanosheet and 1D nanotube morphological conversions presented the good reversibility and repeatability, and the nanosheet exhibited a greater fluorescence enhancement effect than the nanotube.

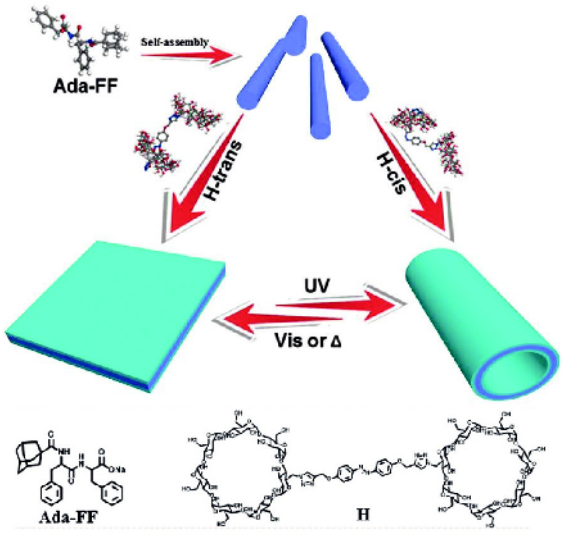

Figure 7 Photo-controlled reversible conversion of nanotube and nanosheets mediated by cyclodextrin dimers (color online).

4 Calixarene/pillararene-based supramolecular systems

Calixarenes and pillararenes are phenol-derived macrocycles mainly bind the neutral or charged fragments of substrates [28]. After modified by ionic groups, the resultant calixarene/pillararene derivatives can reach high water solubility.

Because these calixarene/pillararene derivatives possess three-dimensional, flexible, and significantly π-rich cavities, they are widely used to construct macrocyclic supramolecular systems in aqueous solution. In a typical example, paraquat and diquat, two effective, nonselective, and quick acting viologen herbicides that are used by millions of growers and more than 100 crops in over 120 countries, have high toxicity and long-term formidable risks to human health, society, and the environment. However, their toxicity could effectively be inhibited through a new therapeutic protocol based on the host-guest complexation and charge transfer between calixarene and viologen substrates [29]. That is, owing to the tight binding of paraquat or diquat to the calixarene cavity through electrostatic, π-stacking and especially charge transfer interactions, the interactions of paraquat or diquat with the reducing agents in the cell and the generation of their radical cations became more difficult, which not only decreases the production of the toxic $HO^{\bullet}$ but also deactivates the resulting radicals. As a result, the mortality rate of paraquat was significantly decreased, and the paraquat-induced destruction of tissue structures was prevented, when the poisoned mice were administered with calixarenes (Figure 8(a)). Following this idea, an anionic pillar[6]arene derivative was also used in the therapy of paraquat poisoning through the formation of a stable [2]pseudorotaxane with an extremely high association constant up to 10^8 M^{-1}, leading to less opportunity available for paraquat to interact with the reducing agents in the cell [30]. In another controlled pillararene-viologen supramolucular system, water-soluble pillar[10]arene formed a 1:2 [3]pseudorotaxane with a paraquat derivative (Figure 8(b)). This complexation was cooperative as demonstrated by a Scatchard plot. Furthermore, this pillar[10]arene/paraquat [3]pseudorotaxane self-assembled to a pillararene-based gemini-type supra-amphiphiphile, which converted into vesicles in water above the LCST of a paraquat-containing polymer. Owing to the thermoresponsivenesses of the pillar[10]arene and polymer, as well as their different LCST behaviors, a unique dual-thermoresponsiveness was achieved and further applied in the controlled release of water-soluble dyes calcein and hydrophobic DOX [31].

Interestingly, a water-soluble pillar[5]arene with PEG tails and a targeting moiety biotin as an end group was used to construct an amphiphilic supramolecular assembly with a viologen salt (Figure 9). The binding affinity between pillar[5]arene and viologen decreased significantly by reduction of the dicationic viologen into its cationic radical state due to decreased noncovalent interactions. This assembly could encapsulate the anticancer drug DOX in water and exhibited the reduction-triggered disassembly, resulting in the release of the anticancer drug. The biotin groups decorating the surfaces of the assembly endowed these drug delivery vehicles with excellent targeting ability. *In vitro* experiments showed that these supramolecular carriers delivered the anticancer drug to biotin receptor positive cancer cells. After internalization by the cells, the viologen group was reduced into the cationic radical state by NAD(P)H, resulting in the release of the loaded DOX caused by the disassembly of the assembly. More importantly, the encapsulation of DOX by the assembly retained the therapeutic efficacy of DOX towards cancerous cells, while its cytotoxicity towards normal cells was reduced remarkably. *In vivo* experiments demonstrated that the DOX-loaded assembly exhibited the enhanced accumulation in tumor tissue, dramatically higher antitumor effect and lower systematic toxicity than free DOX in the HeLa tumor xenograft-bearing nude mice [32]. On the other hand, a water-soluble cationic pillar[6]arene could selectively associate with ATP to form a stable 1:1 inclusion complex. As a result, the hydrolysis of ATP was efficiently inhibited in the presence of alkaline phosphatase due to the

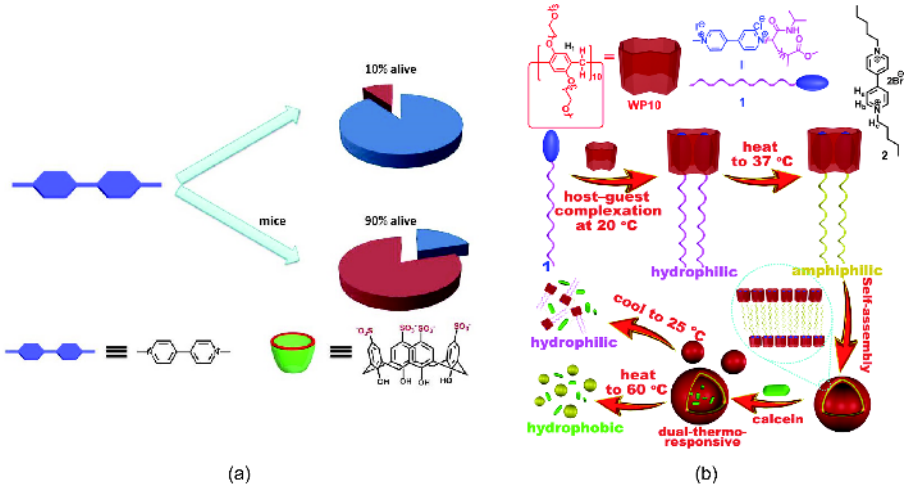

Figure 8 (a) Calixarene-viologen supramolecular assembly and its treatment of viologen poisoning. (b) Pillar[10]arene-viologen supramolecular assembly and its thermo-responsive controlled release (color online).

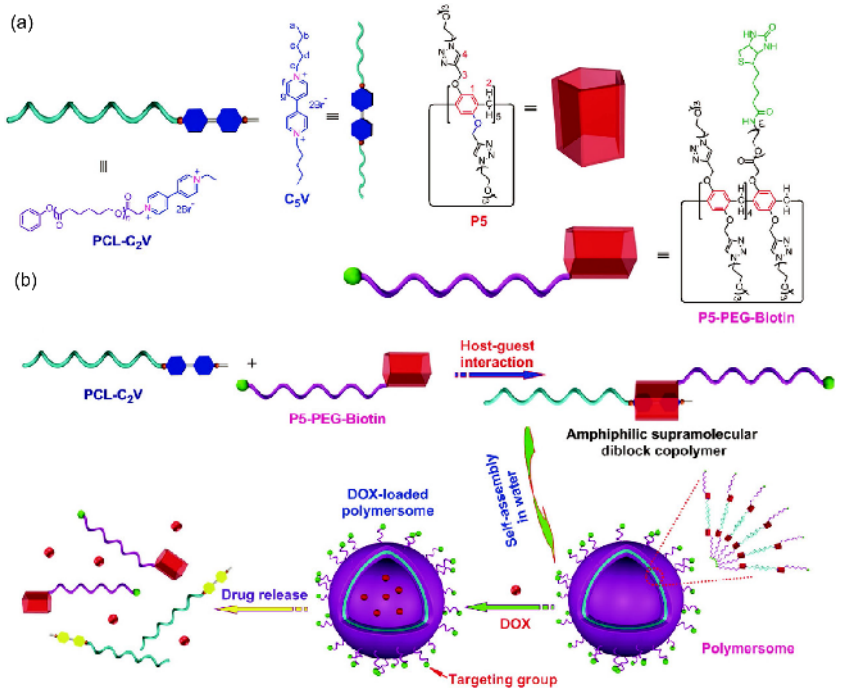

Figure 9 Pillararene-viologen supramolecular assembly and its redox-responsive drug delivery (color online).

existence of a hydrophobic pillar[6]arene cavity. A folic acid ended diblock polymer was further employed to PEGylate the cationic pillar[6]arene to obtain PIC micelles in buffer, endowing them with specific targeting ability to deliver the pillar[6]arene to folate receptor over-expressing cancer cells. The ATP-dependent efflux pump was blocked by cutting off the energy source from ATP hydrolysis due to the formation of the host-guest inclusion complex. Furthermore, MTT assay demonstrated that the efficacy of the anticancer drug DOX·HCl was improved effectively in the presence of PIC micelles. The present results pave a way to develop novel therapeutic agents, implying that supramolecular chemistry may be engineered into promising vehicles to overcome multidrug resistance in cancer therapy. More detailed biologic investigations need to be carried out to figure out the deeper-level mechanism of the MDR treatment [33].

In addition, a CO_2-responsive supramolecular complex was built from a tertiary amine-modified pillar[5]arene and surfactant in water and it was used in the construction of supramolecular vesicles and gas controlled release (Figure 10(a)). With the addition of CO_2, a pillar[5]arene-based host-guest complex formed. Moreover, the formation and destruction of this CO_2-responsive pillar[5]arene-based host-guest complex could be visually judged due to the change of the solution transmittance [34]. By using light irradiation as the external stimulus, a photodegradable anticancer prodrug containing chlorambucil and a fluorophore pyrene moiety and a water soluble pillar[6]arene were utilized to the form a stable host-guest inclusion complex. On the other hand, the release of chlorambucil could be controlled easily by UV irradiation. To improve the membrane permeability, the diblock polymer PEG-*b*-PLKC was employed to form stable

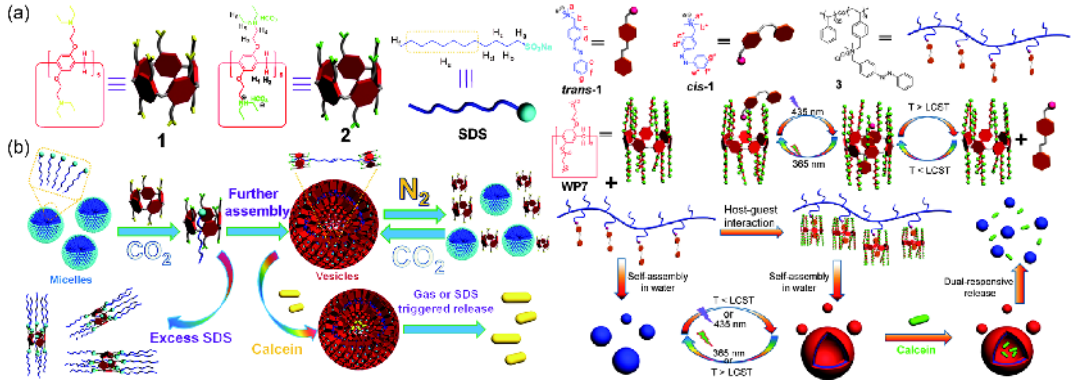

Figure 10 CO_2-responsive and photo/thermo-responsive supramolecular assembly based on water-soluble pillararenes (color online).

ternary polyion complex (PIC) micelles with the pillar[6]arene-prodrug complex and the polylysine segment as the core and the PEG block as the shell. By introducing the non-ionic, bioacceptable and nontoxic hydrophilic PEG into this supramolecular system, the biocompatibility and membrane permeability of the ternary PIC micelles were enhanced significantly. Compared with chlorambucil, the cytotoxicity of the prodrug was decreased effectively by introducing the fluorescent chromophore pyrene as confirmed by MTT assays. Furthermore, the changes in the fluorescence were utilized to indicate loading and unloading of the drug upon photodegradation [35].

Moreover, a supramolecular motif between a water-soluble thermoresponsive pillar[7]arene and an azobenzene guest was established and showed good dual-responsiveness, which was consequently utilized to construct a dual-responsive supra-amphiphilic polypseudorotaxane in water (Figure 10(b)). Due to the thermoresponsiveness of pillar[7]arene and photoresponsiveness of the azobenzene unit, the reversible transformations between solid nanospheres based on the self-assembly of the polymer backbone and vesicles based on the self-assembly of the supra-amphiphilic polypseudorotaxane were achieved by adjusting the solution temperature or UV-visible light irradiation. Therefore, the vesicles were further used in the controlled release of water-soluble dye calcein molecules [36].

In addition to controlled release systems, water-soluble pillararenes have been also used to construct other functional supramolecular systems. A typical example comes from near-infrared emission (NIE)-active nanoparticles fabricated by employing the host-guest complex of a water-soluble pillar[5]arene as a building block (Figure 11). Without pillar[5]arene, the nanoribbons self-assembled from the guest dye showed relatively weak fluorescence emission. However, the nanoparticles showed very strong NIR fluorescence emission at low concentrations because of the host-guest complexation-enhanced aggregation. Furthermore, these nanoparticles were utilized as an imaging agent for living cells due to their NIR emission. These results indicated that pillararene-based host-guest complexes may have enormous potential in biological and pharmaceutical fields, including cell imaging and biosensors [37]. Alternatively, pillar[5]arene could also enhance the aggregation-induced emission of a tetraphenylethene (TPE) derivative through the supramolecular assembly. Upon the formation of the assembly, the fluorescence emission of the TPE-based fluorogen was enhanced effectively, because the intramolecular rotation of aromatic rings of TPE group was restricted and the nonradiative decay channels were blocked effectively by the formation of a [2]pseudorotaxane-type structure. Through the reprecipitation technique, nanoparticles with an average diameter of 43 nm were obtained, which could be utilized as an imaging agent to light up the cells [38].

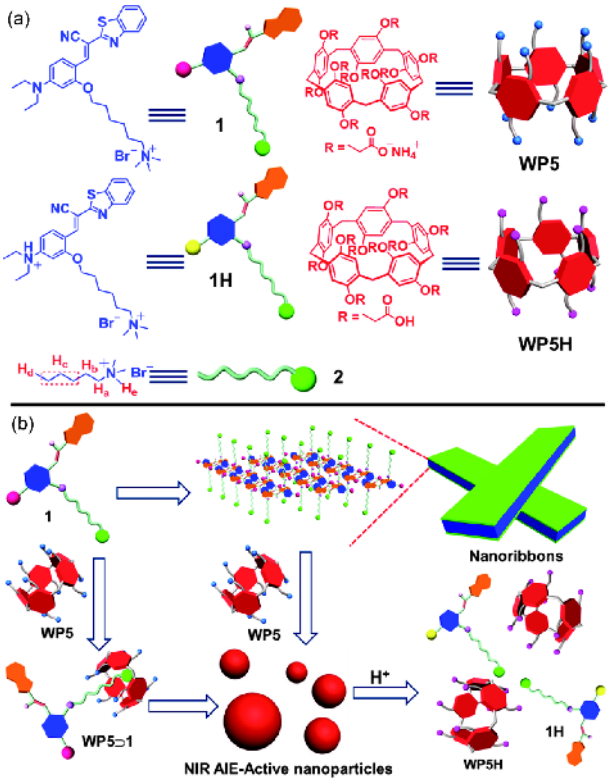

Figure 11 Nanoparticles with near-infrared emission enhanced by pillararene-based supramolecular assembly in water (color online).

5 Cucurbituril-based supramolecular systems

Cucurbiturils, a class of macrocycles comprising 5-10 glycoluril units, have a hydrophobic cavity and two identical carbonyl-laced portals, which allow them to form stable inclusion complexes with a wide variety of cationic guest molecules [39−50]. In the cucurbituril family, cucurbit[8]uril has a cavity comparable to that of γ-cyclodextrin and exhibits remarkable host-guest properties different from those of smaller cucurbiturils. Significantly, cucurbit[8]uril can include two guest molecules inside its cavity to form a stable 1:2 complex [51]. Hydrophobically driven encapsulation of the homodimers of the 4,4′-bipyridine (BP) unit on the peripheral pyridine rings of the rigid stacking-forbidden triangular 1,3,5-triphenylbenzene compound in the cavity of the CB[8] hold the monomers together in 2D space to form the first homogeneous supramolecular organic framework (SOF) in water (Figure 12) [52]. Currently, this strategy has been utilized to generate other 2D supramolecular organic frameworks [53−65].

The generation of the 2D SOFs showed the robustness of CB[8]-encapsulation-promoted dimerization of aromatic units in aqueous media. Intermolecular stacking of the peripheral 4-(4-methoxyphenyl)pyridin-4-ium (PP) units on tetrahedral tetra(4-methylenephenyl)methane was promoted

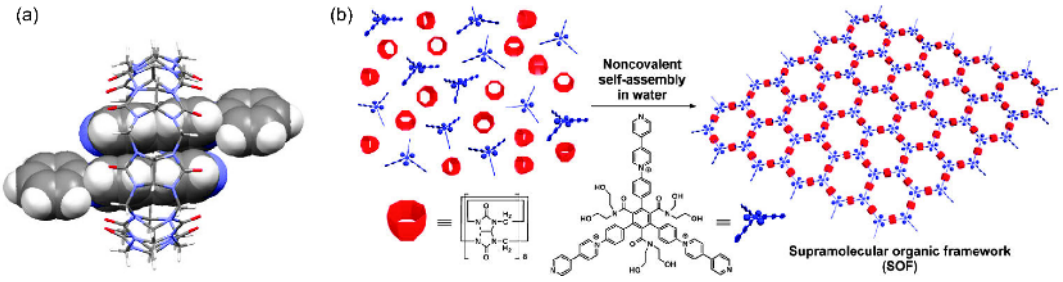

Figure 12 (a) Crystal structure of the 2:1 complex between 1-phenyl-BP and CB[8]. (b) Schematic representation of the self-assembly of peripheral BP substituted triangular 1,3,5-triphenylbenzene derivative with CB[8] in water to form 2D honeycomb SOF (color online).

by CB[8] to construct a novel water soluble 3D SOF material (Figure 13) [66]. The 1:2 mixture of the tetramer **PPTetra**(OMe) with CB[8] exhibited high complexation stability with apparent association constant (K_a) up to 1.3×10^{14} M^{-2} in 50 mM CD_3CO_2Na-buffered D_2O determined with the competition ^1H NMR method. Under the same analysis conditions, the K_a values of the 2:1 complexes between the PhPy units of various substituents, such as SMe, NMe_2, CN, CH_2OH and CHO, with CB[8] were comparable to that of 3D SOF formed from **PPTetra**(OMe) and CB[8], which means the construction of the 3D SOF was, to a considerable extent, substituent-independent [67−70]. DLS experiments showed that the concentration-dependent D_H values were time-independent, indicating the quick generation of 3D SOF. Solution-phase small-angle X-ray scattering and diffraction experiments demonstrate that the encapsulations of every two aromatic units within cucurbit[8]uril directly co-assemble a tetratopic molecular block into a periodic 3D SOF in water.

The void volume of the above 3D SOFs was assessed to be 77% and the pore aperture, defined by the six CB[8] units in one self-assembled macrocycle which adopts a cyclohexane-like chair conformation, was estimated to be about 2.1 nm. The polycationic 3D SOF could efficiently absorb various anionic organic guests, including **Dye-1**–**6**, ***s*DNA-1**–**4**, **DNA-1**–**2**, **PAMAM-1**–**3**, **Peptide-1**–**4**, and **Drug-1**–**5**, based on "hard and soft acids and bases" theory (Figure 14) [66]. In virtue of low cytotoxicity and a nano-scale range for the homogeneous 3D SOFs, which is very suitable for cell uptake due to electron paramagnetic resonance (EPR) effect, such periodic porous SOFs have been further explored as drug delivery systems (DDSs) (Figure 15) [68,69].

Fluorescence titration experiments showed that efficient absorption of pemetrexed disodium (PMX, **Drug-4**) by the polyelectrolyte framework SOF(SMe) occurred quickly in phosphate-buffered saline (PBS) at physiological pH 7.4 [68]. It was confirmed by DLS analysis that the frameworks were maintained after absorption of PMX. Regular porosity of the SOFs was believed to minimize electrostatic repulsion of the PMX anions. Most of the drug was retained within the frameworks at normal blood plasma pH of 7.4, while release of PMX were happened much more quickly at pH 4.5. Further studies demonstrated that PMX-loaded SOF (PMX@SOF) could be internalized in multidrug resistance (MDR) MCF-7/Adr cells via an energy-dependent endocytosis process mediated by clathrin [68]. *In vitro* and *in vivo* studies have revealed that sof-DDSs considerably improve the treatment efficacy to PMX, leading to 6–12-fold reduction of the IC_{50} values. It was also manifested that the delivery capability of the drug-loaded SOF depended mainly

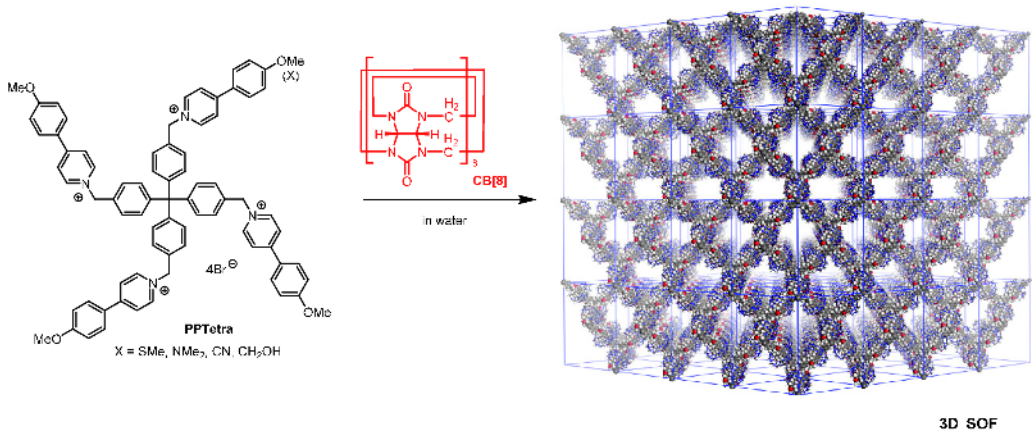

Figure 13 Self-assembly of tetratopic molecular blocks into a periodic three-dimensional supramolecular organic framework (3D SOF) in water (color online).

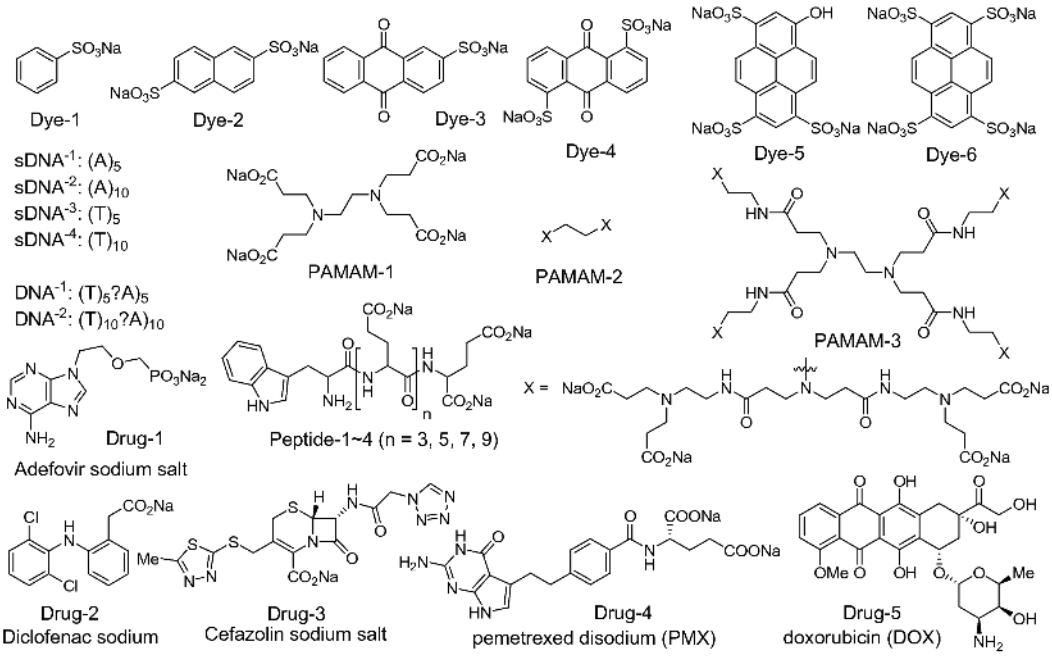

Figure 14 The structures of **Dye-1–6**, ***s*DNA-1–4**, **DNA-1–2**, **PAMAM-1–3**, **Peptide-1–4**, and **Drug-1–5** (color online).

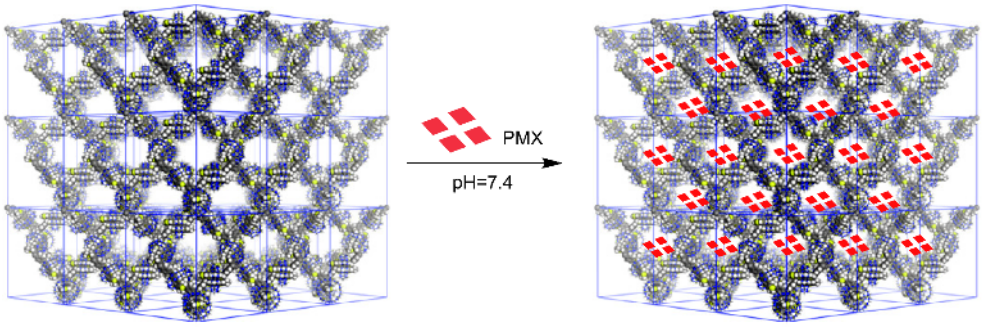

Figure 15 Illustration of the absorption of PMX by the self-assembled 3D SOF(SMe) in pH 7.4 (color online).

on the interior porous of SOFs, whereas the substituents on the peripheral phenyl ring of the tetrahedral monomers imposed unremarkable influence. Moreover, doxorubicin (DOX, **Drug-5**), a clinically widely used neutral hydrophobic chemotherapeutic drug, could be adsorbed by the diamondoid SOF-based DDSs with hydrophobicity as the exclusive driving force and maintained in aqueous media at the physiological pH of 7.4. In acidic MDR MCF-7/Adr cancer cells the adsorbed DOX in SOF was released readily via protonation of the amino group of the drug to kill the cancer cells with remarkably improved efficacy in both *in vitro* and *in vivo* studies. This new SOF-DDSs strategy omits the indispensable loading process required by most of reported nano-scaled carriers for neutral hydrophobic chemotherapeutic agents, and thus should be highly valuable for future development of low-cost delivery systems.

While tetratopic molecular block was changed to other kind of building blocks, self-assembly strategy can be used to create various complicated, ordered supramolecular architectures under mild conditions. A successful example is the self-assembled generation of the first homogeneous supramolecular metal-organic framework (SMOF) in water at room temperature from a hexaarmed $[Ru(bpy)_3]^{2+}$-based precursor and CB[8] (Figure 16) [71−73]. The periodic cubic structure in solution of this transition metal-cored supramolecular organic framework is confirmed by small-angle X-ray scattering and diffraction experiments, and also supported by TEM imaging in the solid state. Thus the self-assembled frameworks SMOF possess periodicity and porosity structure in both solution and the solid state, which advantages over MOFs. The void volume of cubic SMOF was estimated to be 80% and the pore aperture was calculated to be about 1.5 nm, defined by the four CB[8] units in one self-assembled macrocycle adopting a square-like conformation. Redox-active Wells-Dawson-type polyoxoanions $[P_2W_{18}O_{62}]^{6-}$ (WD-POM), which has a size of about 1.1 nm,

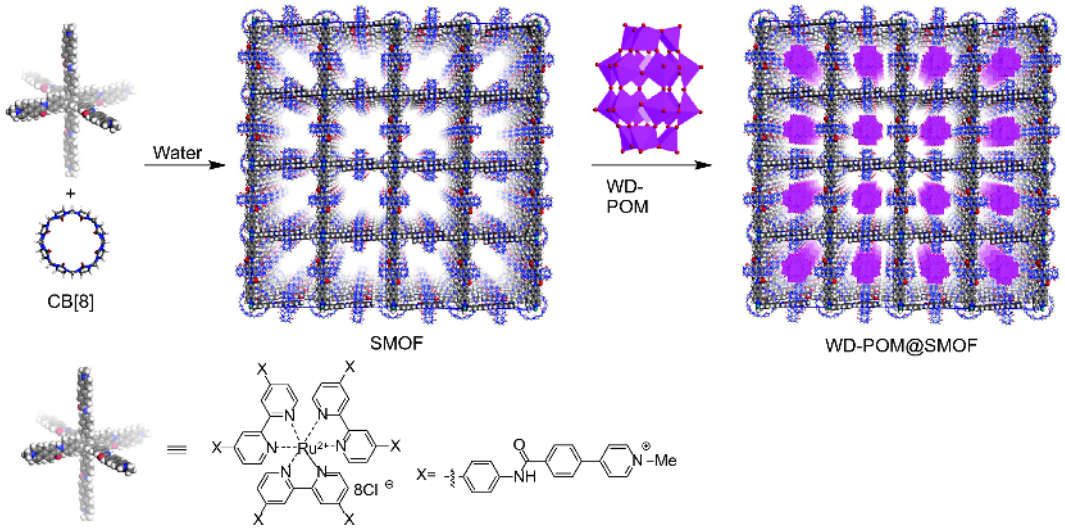

Figure 16 Self-assembly of 3D cubic SMOF and WD-POM loading (color online).

could be encapsulated in the 3D cubic SMOF in one-cage-one-POM manner in water. SAXS and XRD analysis indicated that POM-loaded SMOF maintained its periodicity in both water and at the solid state. It was found that on 500 nm visible light excitation in acidic aqueous solution (pH=1.8) using MeOH as a sacrificial electron donor, H_2 production of WD-POM@SMOF system is about 4 times higher than that of a heterogeneous WD-POM@$[Ru(bpy)_3]^{2+}$-MOF system containing the identical amounts of WD-POM and Ru(II) units. WD-POM@SMOF system facilitates fast multi-electron injection from the $[Ru(bpy)_3]^{2+}$ units to the encapsulated WD-POM anions, leading to substantially efficient hydrogen production. The unique one-cage-one-POM arrangement and homogeneity of the system contribute to the high efficiency, which was also revealed by a Ru^{2+}-derived metal-covalent-supramolecular organic framework [72,73]. Such new porous frameworks may be used to tune the photophysical and photochemical properties of functionalized nanoparticles through encapsulation. New functions and properties will be developed by functionalized the building blocks of SMOF or post-modifications.

6 Conclusions and outlook

It is clear that the controlled supramolecular assembly can contribute to the construction of macrocyclic nanostructures via van der Waals, hydrogen bond, hydrophobic, electrostatic interactions, etc., and the macrocyclic supramolecular systems thus obtained always exhibit significantly improved binding abilities and the fascinating properties, which enable many successful material and biological applications of macrocyclic supramolecular systems. In this review it has been shown that there are many successful examples of macrocyclic supramolecular systems with assembly/disassembly, morphological conversion, and luminescent/drug delivery behaviors in aqueous environment, and these behaviors can be efficiently controlled through the smart adjustment of external stimuli, such as light irradiation, temperature, acid/base, and redox. In this regard, the guiding principle for designing controllable macrocyclic supramolecular assembly can be approved in the light of accumulated research accomplishments summarized here, and an important target of the forthcoming studies on functional supramolecular systems may be to establish the well-organized water-soluble and controllable supramolecular systems through the judicious selection and alignment of substituent on macrocycle rims and the substrate included in the macrocycle cavity to construct efficient supramolecular luminescent materials and probes, supramolecular drug delivery systems, as well as supramolecular bioactive materials. Significantly, the non-covalent nature and multistimuli responsive properties will enable not only the convenient, detachable and dynamic construction but also the intelligent control strategy of the macrocyclic supramolecular systems. Past two decades witnessed a significant harvest in water-soluble and controllable macrocyclic supramolecular systems, and the need for functional materials that requires good properties provides timely opportunities for the application of macrocyclic supramolecular systems. Therefore, we believe that exciting findings and potentials of macrocyclic supramolecular systems are only beginning to be discovered.

Acknowledgements This work was supported by the National Natural Science Foundation of China (91527301, 21432004)

Conflict of interest The authors declare that they have no conflict of interest.

1 (a) Liu Z, Nalluri SKM, Stoddart JF. *Chem Soc Rev*, 2017, 46: 2459–2478; (b) Yu G, Jie K, Huang F. *Chem Rev*, 2015, 115: 7240–7303; (c) Qi Z, Schalley CA. *Acc Chem Res*, 2014, 47: 2222–2233
2 (a) Qu DH, Wang QC, Zhang QW, Ma X, Tian H. *Chem Rev*, 2015, 115: 7543–7588; (b) Yan X, Wang F, Zheng B, Huang F. *Chem Soc Rev*, 2012, 41: 6042–6065; (c) Yang YW, Sun YL, Song N. *Acc Chem Res*, 2014, 47: 1950–1960
3 (a) Amabilino DB, Stoddart JF. *Chem Rev*, 1995, 95: 2725–2828; (b) Erbas-Cakmak S, Leigh DA, McTernan CT, Nussbaumer AL. *Chem Rev*, 2015, 115: 10081–10206
4 Vella SJ, Tiburcio J, Gauld JW, Loeb SJ. *Org Lett*, 2006, 8: 3421–3424
5 Murakami Y, Kikuchi J, Hisaeda Y, Hayashida O. *Chem Rev*, 1996, 96: 721–758
6 (a) Balzani V, Credi A, Raymo F, Stoddart J . *Angew Chem Int Ed*, 2000, 39: 3348–3391; (b) Balzani V, Gómez-López M, Stoddart JF. *Acc Chem Res*, 1998, 31: 405–414
7 (a) Blanco MJ, Consuelo Jiménez M, Chambron JC, Heitz V, Linke M, Sauvage JP. *Chem Soc Rev*, 1999, 28: 293–305; (b) Sauvage JP. *Acc Chem Res*, 1998, 31: 611–619
8 Jiang W, Han M, Zhang HY, Zhang ZJ, Liu Y. *Chem Eur J*, 2009, 15: 9938–9945
9 Liu Y, Han M, Zhang HY, Yang LX, Jiang W. *Org Lett*, 2008, 10: 2873–2876
10 Suresh M, Mandal AK, Suresh E, Das A. *Chem Sci*, 2013, 4: 2380–2386
11 Xu H, Rudkevich DM. *J Org Chem*, 2004, 69: 8609–8617
12 (a) Liu Y, Flood AH, Bonvallet PA, Vignon SA, Northrop BH, Tseng HR, Jeppesen JO, Huang TJ, Brough B, Baller M, Magonov S, Solares SD, Goddard WA, Ho CM, Stoddart JF. *J Am Chem Soc*, 2005, 127: 9745–9759; (b) Aprahamian I, Olsen JC, Trabolsi A, Stoddart JF. *Chem Eur J*, 2008, 14: 3889–3895
13 Jiang Q, Zhang HY, Han M, Ding ZJ, Liu Y. *Org Lett*, 2010, 12: 1728–1731
14 (a) Gokel GW, Leevy WM, Weber ME. *Chem Rev*, 2004, 104: 2723–2750; (b) Li J, Yim D, Jang WD, Yoon J. *Chem Soc Rev*, 2017, 46: 2437–2458; (c) Zheng B, Wang F, Dong S, Huang F. *Chem Soc Rev*, 2012, 41: 1621–1636
15 (a) Hoffart DJ, Tiburcio J, de la Torre A, Knight LK, Loeb SJ. *Angew Chem Int Ed*, 2008, 47: 97–101; (b) Lestini E, Nikitin K, Müller-Bunz H, Fitzmaurice D. *Chem Eur J*, 2008, 14: 1095–1106
16 Wang J, Zhang HY, Zhang XJ, Song ZH, Zhao XJ, Liu Y. *Chem Commun*, 2015, 51: 7329–7332
17 Wang J, Zhang YM, Zhang XJ, Zhao XJ, Liu Y. *Asian J Org Chem*, 2015, 4: 244–250
18 Zhang W, Zhang YM, Li SH, Cui YL, Yu J, Liu Y. *Angew Chem Int Ed*, 2016, 55: 11452–11456
19 (a) Lai WF, Rogach AL, Wong WT. *Chem Soc Rev*, 2017, 46: 6379–6419; (b) Szejtli J. *Chem Rev*, 1998, 98: 1743–1754; (c) Crini G. *Chem Rev*, 2014, 114: 10940–10975
20 Rekharsky MV, Inoue Y. *Chem Rev*, 1998, 98: 1875–1918
21 Chen Y, Liu Y. *Chem Soc Rev*, 2010, 39: 495–505
22 (a) Uekama K, Hirayama F, Irie T. *Chem Rev*, 1998, 98: 2045–2076; (b) Zhao Q, Chen Y, Liu Y. *Chin Chem Lett*, 2018, 29: 84–86; (c) Liang L, Chen Y, Chen XM, Zhang Y, Liu Y. *Chin Chem Lett*, 2018, 29: 989–991
23 Breslow R, Dong SD. *Chem Rev*, 1998, 98: 1997–2012
24 Li JJ, Chen Y, Yu J, Cheng N, Liu Y. *Adv Mater*, 2017, 29: 1701905
25 Zhang YM, Han M, Chen HZ, Zhang Y, Liu Y. *Org Lett*, 2013, 15: 124–127
26 Sun HL, Chen Y, Zhao J, Liu Y. *Angew Chem Int Ed*, 2015, 54: 9376–9380
27 Sun HL, Chen Y, Han X, Liu Y. *Angew Chem Int Ed*, 2017, 56: 7062–7065
28 (a) Guo DS, Liu Y. *Chem Soc Rev*, 2012, 41: 5907–5921; (b) Gutsche CD, Dhawan B, No KH, Muthukrishnan R. *J Am Chem Soc*, 1981, 103: 3782–3792; (c) Xue M, Yang Y, Chi X, Zhang Z, Huang F. *Acc Chem Res*, 2012, 45: 1294–1308; (d) Ogoshi T, Yamagishi TA, Nakamoto Y. *Chem Rev*, 2016, 116: 7937–8002
29 Wang K, Guo DS, Zhang HQ, Li D, Zheng XL, Liu Y. *J Med Chem*, 2009, 52: 6402–6412
30 Yu G, Zhou X, Zhang Z, Han C, Mao Z, Gao C, Huang F. *J Am Chem Soc*, 2012, 134: 19489–19497
31 Chi X, Yu G, Shao L, Chen J, Huang F. *J Am Chem Soc*, 2016u, 138: 3168–3174
32 Yu G, Yu W, Shao L, Zhang Z, Chi X, Mao Z, Gao C, Huang F. *Adv Funct Mater*, 2016, 26: 8999–9008
33 Yu G, Zhou J, Shen J, Tang G, Huang F. *Chem Sci*, 2016, 7: 4073–4078
34 Jie K, Zhou Y, Yao Y, Shi B, Huang F. *J Am Chem Soc*, 2015, 137: 10472–10475
35 Yu G, Yu W, Mao Z, Gao C, Huang F. *Small*, 2015, 11: 919–925
36 Chi X, Ji X, Xia D, Huang F. *J Am Chem Soc*, 2015, 137: 1440–1443
37 Shi B, Jie K, Zhou Y, Zhou J, Xia D, Huang F. *J Am Chem Soc*, 2016, 138: 80–83
38 Zhou J, Hua B, Shao L, Feng H, Yu G. *Chem Commun*, 2016, 52: 5749–5752
39 Kim K, Selvapalam N, Ko YH, Park KM, Kim D, Kim J. *Chem Soc Rev*, 2007, 36: 267–279
40 Yang X, Liu F, Zhao Z, Liang F, Zhang H, Liu S. *Chin Chem Lett*, 2018, http://doi.org/101016/jcclet201801032
41 Kuok KI, Li S, Wyman IW, Wang R. *Ann NY Acad Sci*, 2017, 1398: 108–119
42 Tian J, Zhang L, Wang H, Zhang DW, Li ZT. *Supramol Chem*, 2016, 28: 769–783
43 Ni XL, Xiao X, Cong H, Zhu QJ, Xue SF, Tao Z. *Acc Chem Res*, 2014, 47: 1386–1395
44 Bai D, Wang X, Gao Z, Qiu S, Tao Z, Zhang J, Xiao X. *Chin J Org Chem*, 2017, 37: 2022–2027
45 Yin ZJ, Wu ZQ, Lin F, Qi QY, Xu XN, Zhao X. *Chin Chem Lett*, 2017, 28: 1167–1171
46 Wu W, Song S, Cui X, Sun T, Zhang JX, Ni XL. *Chin Chem Lett*, 2018, 29: 95–98
47 Li B, Li X, Sun X, Wang N. *Chin J Chem*, 2016, 34: 1114–1120
48 Li TT, Wen LL, Ji HL, Liu FY, Sun SG. *Chin Chem Lett*, 2017, 28: 463–466
49 Zhang M, Gao J, Chen J, Cai M, Jiang J, Tian Z, Wang H. *Sci China Chem*, 2016, 59: 848–852
50 Cui XW, Chen SY, Wang CZ, Zhao WX, Sun T, Ni XL, Zhang YQ, Tao Z. *Chin Chem Lett*, 2016, 27: 173–177
51 Liu Y, Yang H, Wang Z, Zhang X. *Chem Asian J*, 2013, 8: 1626–1632
52 Zhang KD, Tian J, Hanifi D, Zhang Y, Sue ACH, Zhou TY, Zhang L, Zhao X, Liu Y, Li ZT. *J Am Chem Soc*, 2013, 135: 17913–17918
53 Zhang L, Zhou TY, Tian J, Wang H, Zhang DW, Zhao X, Liu Y, Li ZT. *Polym Chem*, 2014, 5: 4715–4721
54 Xu SQ, Zhang X, Nie CB, Pang ZF, Xu XN, Zhao X. *Chem Commun*, 2015, 51: 16417–16420
55 Pfeffermann M, Dong R, Graf R, Zajaczkowski W, Gorelik T, Pisula W, Narita A, Müllen K, Feng X. *J Am Chem Soc*, 2015, 137: 14525–14532
56 Zhang Y, Zhan TG, Zhou TY, Qi QY, Xu XN, Zhao X. *Chem Commun*, 2016, 52: 7588–7591
57 Lee HJ, Kim HJ, Lee EC, Kim J, Park SY. *Chem Asian J*, 2018, 13: 390–394
58 Lin Q, Fan YQ, Mao PP, Liu L, Liu J, Zhang YM, Yao H, Wei TB. *Chem Eur J*, 2018, 24: 777–783
59 Li Y, Dong Y, Miao X, Ren Y, Zhang B, Wang P, Yu Y, Li B, Isaacs L, Cao L. *Angew Chem Int Ed*, 2018, 57: 729–733
60 H Wang, D W Zhang, Z T Li. *Acta Polym Sin*, 2017, 1: 19–26
61 Tian J, Chen L, Zhang DW, Liu Y, Li ZT. *Chem Commun*, 2016, 52: 6351–6362
62 Wang H, Zhang D, Zhao X, Li Z. *Acta Chim Sin*, 2015, 73: 471–479
63 Zhang L, Jia Y, Wang H, Zhang DW, Zhang Q, Liu Y, Li ZT. *Polym Chem*, 2016, 7: 1861–1865

64 Zhang X, Nie CB, Zhou TY, Qi QY, Fu J, Wang XZ, Dai L, Chen Y, Zhao X. *Polym Chem*, 2015, 6: 1923–1927
65 Madasamy K, Shanmugam VM, Velayutham D, Kathiresan M. *Sci Rep*, 2018, 8: 1354
66 Tian J, Zhou TY, Zhang SC, Aloni S, Altoe MV, Xie SH, Wang H, Zhang DW, Zhao X, Liu Y, Li ZT. *Nat Commun*, 2014, 5: 5574–5584
67 Yu SB, Qi Q, Yang B, Wang H, Zhang DW, Liu Y, Li ZT. *Small*, 2018, 14: 1801037
68 Tian J, Yao C, Yang WL, Zhang L, Zhang DW, Wang H, Zhang F, Liu Y, Li ZT. *Chin Chem Lett*, 2017, 28: 798–806
69 Yao C, Tian J, Wang H, Zhang DW, Liu Y, Zhang F, Li ZT. *Chin Chem Lett*, 2017, 28: 893–899
70 Wu YP, Yang B, Tian J, Yu SB, Wang H, Zhang DW, Liu Y, Li ZT. *Chem Commun*, 2017, 53: 13367–13370
71 Tian J, Xu ZY, Zhang DW, Wang H, Xie SH, Xu DW, Ren YH, Wang H, Liu Y, Li ZT. *Nat Commun*, 2016, 7: 11580
72 Li XF, Yu SB, Yang B, Tian J, Wang H, Zhang DW, Liu Y, Li ZT. *Sci China Chem*, 2018, https://doi.org/10.1007/s11426-018-9234-2
73 Tian J, Wang H, Zhang DW, Liu Y, Li ZT. *Natl Sci Rev*, 2017, 4: 426–436